Brodogradnja/Shipbuilding/Open access Volume 73 Number 4, 2022

David Ricardo Alvarado
Luis Alejandro Paternina
Edwin Giovanny Paipa

http://dx.doi.org/10.21278/brod73402

ISSN 0007-215X
eISSN 1845-5859

SYNTHESIS MODEL FOR THE CONCEPTUAL DESIGN OF INLAND CARGO VESSELS TO OPERATE ON THE MAGDALENA RIVER

UDC 656.629:629.5.01
Original scientific paper

Summary

Inland waterways are presented both as a need and an opportunity for developing an intermodal transport system to boost Colombian economic growth. Riverine transportation as part of an intermodal system represents conveying a significant amount of cargo at a low cost and therefore reducing greenhouse gas emissions. To competitively include this cargo transportation alternative in an intermodal context, the development of effective container vessels is required. Most of the Colombian rivers present sedimentary, high flow, and low depth nature. Then, the design of riverine cargo vessels capable of navigating in shallow waters with less brake power requirements is needed. A synthesis model: an automatic and integrated design procedure, has been programmed to generate and evaluate feasible vessel dimensions at a conceptual design stage. Through systematic variations of the main dimensions, this procedure allows evaluating a design space in which the most effective concept-vessel solution is selected. At the end of this procedure, the main characteristics for container vessels in the Magdalena River at a conceptual design stage, are defined. Validation of the synthesis model with a riverine logistic support ship is provided.

Keywords: Riverine cargo vessels; conceptual design; synthesis model

Nomenclature

L_{OA}	Length overall	P_E	Effective power	C_{out}	Outfitting Cost
L	Length at waterline	P_B	Brake power	$C_{m/c}$	Propulsion plant costs
B	Molded beam	Fn_h	Depth Froude number	C_{Slab}	Labor Cost
D	Depth	η_{prop}	Propulsive efficiency	C_0	Unit cost of the material
T	Draught	GMT	Metacentric height	C_{olab}	Labor equipment cost
C_b	Block coefficient	BMT	Metacentric radius	Cmh_{hull}	Hull construction man hour cost
A_m	Midship section surface	KG_{steel}	Steel centre of gravity	C_{omat}	Equipment material cost
V	Ship speed	KG_{out}	Outfitting centre of gravity	Cmh_{out}	Outfitting man hours cost
h	River depth	$KG_{m/c}$	Machinery centre of gravity	Mhs_{out}	Outfitting man hours
Dwt	Deadweight	KG_{cont}	Container centre of gravity	Mhs_{Hull}	Man hours for hull construction
W_{light}	Lightweight	N_{Layer}	Layers of containers	S_v	Steel waste factor
W_{Steel}	Structural weight	hcn	Container height	V_{steel}	Steel cost per tonne
W_{out}	Outfitting weight	C_{Req}	Construction cost	Δ	Displacement
$W_{m/c}$	Machinery weight	C_{Steel}	Steel cost	ρ_0	Water density
RT	Total hull resistance	C_{Smat}	Material Cost	T_w	Tank water temperature

1. Introduction

From colonial times to the first decades of the XX century, the Magdalena River had been the main way of transport for imported goods and routes for immigrants heading to the inland cities. Nevertheless, the construction of railways and roads, the strengthening of the airways, and the loss of the river's navigability mean that the cargo transportation by this river is relegated to government oblivion. At the end of XX century, the cargo and passenger conveyance by this river was mostly represented by tugboats and small high-speed crafts. Studies have been done to make navigation on the Magdalena River a key part of the country's plan for a multimodal transportation system.

Colombia is facing the challenge of connecting the national economic activities while energy and environmental impacts are under the allowed levels established by several international treaties related to climate change. Even though the lower operational costs are associated with rail and river modes of transport, currently, most of the cargo and passenger transportation is by paved roads, 64% of the once well-extended Colombian railway system is nowadays inactive and most of the river transport infrastructure is obsolete.

In fluvial transportation, there are four main basins with a total of 18225 km of navigable waterways. The Magdalena is the one with the highest volume of cargo and passenger transportation [1]. Currently, given sedimentary processes in rivers and the decadent infrastructure of mostly wharves and piers, the conditions are not adequate to reactivate the navigation on these rivers on a larger scale. Therefore, the Colombian government has launched a plan to generate a road map detailing the steps to include inland waterways in a multimodal transport system. One of the topics is to define a vessel capable of navigating in rivers of sedimentary high flow and depths from 2.0 m to 20 m. This vessel class's design must also take into account minimizing installed brake power and weight.

To design a class of inland waterway container vessels to fulfil the requirements requested, such as the capability of navigating in shallow waters with fewer brake power requirements, first it is necessary to convert all the requirements into technical information. At this stage, the basic vessel's characteristics such as length, beam, draft, or brake power are established. On this basis, the following design stages are developed in an iterative process until a vessel that satisfies all the requirements is generated. These approaches are known as 'point-based design', the result obtained only occupies a single point in the scenario of possible solutions. Kerns [2] stated that the traditional approach to vessel design is largely an 'ad hoc' process based on experience, design lines, and rules of thumb where, often, objective attributes are not adequately quantified to support efficient and effective decisions. Then, even though after the design cycle is finished and an effective vessel has been designed, a possibility exists that a better performing vessel could have been developed. For the reasons previously explained, a vessel synthesis model is proposed to obtain the basic characteristics of the most effective vessel at a conceptual stage.

The development of a cargo vessel with such performance requires the elaboration of a great amount of data, most of which are strongly interdependent, just as in the case of hull weight, resistance, and the brake power required. Then, the interdependence of input data implies that it is not possible to analyse and solve each problem separately without establishing a time-consuming iterative process [3]. Therefore, an automatic design method is highly beneficial for exploring a large number of different design combinations.

In the synthesis model procedure, a parent hull shape is adopted to evaluate, through systematic variations of the main dimensions, all the elements necessary to perform the classical steps of the design. Some parts of the conceptual model have been calibrated with data from existing vessels, to ensure accuracy in the predictions [4]. In the end, a group of possible conceptual vessel solutions with a wide variety of dimensions and technical characteristics are obtained. Each solution is evaluated, and, according to the design's requirements, these solutions are ranked based on measures of merit criteria.

This work intends to define the main characteristics at a conceptual design stage of a riverine container cargo vessel, capable of operating in the Magdalena River through a vessel synthesis model. Next, the structure of the synthesis model algorithm is explained.

2. Synthesis model conceptual design process

In order to obtain the riverine vessel's convenient dimensions and desirable characteristics as a first step to developing a complete and functional design, the workflow shown in Fig. 1 is followed. First, restrictions are given by the river and the functional requirements of the desired vessel are clarified. Then, a group of possible conceptual vessel solutions with a wide variety of dimensions and technical characteristics is obtained. Those solutions give rise to a design space in which frontiers are given by the river dimensions and functional restrictions. Finally, the obtained results are ranked by the measure of merit criteria. The best-ranked vessel dimensions could be the basis for later design stages.

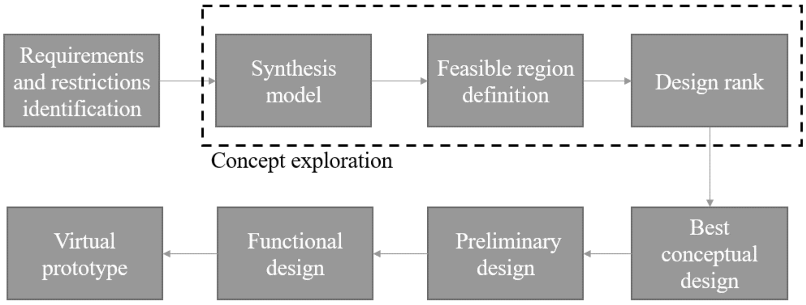

Fig. 1 Flowchart of the integrated design process

First, input design parameters, such as length, beam, draught, and block coefficient are defined. From each of these combinations, technical characteristics such as lightweight, payload capabilities, powering and stability calculations are performed. Only if the results of these characteristics are feasible and present a convergence among the interdependent modules, the acquisition cost is calculated, and the alternative is stored [see Fig. 2].

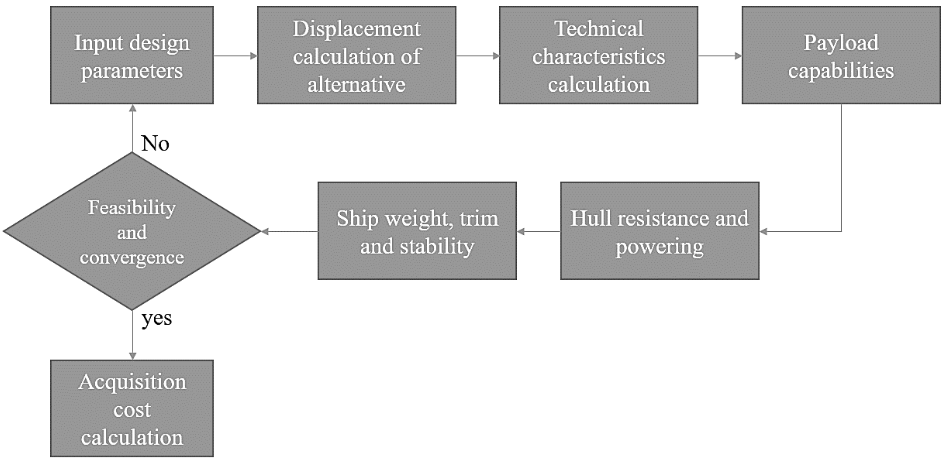

Fig. 2 Flowchart of the synthesis model vessel generation and check

The model is divided into five different modules. Each represents a set of naval architecture analytical and semi-empirical models. Each model will be explained in the following section.

2.1 Weight checking computation module

Balance between lightweight and displacement is a pivotal constraint in the synthesis model. This balance allows to rule out the alternatives that do not converge and, hence, are not part of the feasible region. This constraint is expressed as follows [see Eq.1].

$$L * B * T * C_{\text{B}} * \rho_0 - W_{\text{light}} - Dwt = 0 \tag{1}$$

2.2 Resistance and powering computation module

Brake power estimation, at this stage of the design, might be inaccurate given the hull's forms and hull-propulsion system relation vessel are slightly defined [5]. Despite the vast body of research into hull resistance models, most of them are focused on marine vessels and due to high block coefficients with high L/B ratios typical of inland waters vessels, these models are not considered [4] [6]. Schneekluth & Bertram proposed [7] a semi-empirical relation between displacement, hull resistance, and velocity for inland vessels' preliminary designs on deep waters. In order to calculate the total hull resistance (*RT*), a polynomial regression was applied [see Eq. 2].

$$\frac{RT}{\Delta} = 73.73\left(\frac{\text{V}}{\sqrt{L}}\right)^4 - 144.9\left(\frac{\text{V}}{\sqrt{L}}\right)^3 + 115.9\left(\frac{\text{V}}{\sqrt{L}}\right)^2 - 28.87\left(\frac{\text{V}}{\sqrt{L}}\right) + 2.99\ \frac{lbf}{t} \tag{2}$$

Since inland ships usually navigate in restricted-depth waters, certain changes occur due to the interaction between the vessel and the riverbed [8]. In the first place, there is an effective increase in velocity and, by Bernoulli's principle, a decrease in pressure under the hull, resulting in significant changes in sinkage and trim. This leads to friction drag and wave resistance increments.

At low speeds, the depth of water does not affect the wave pattern, nevertheless, by increasing the vessel speed above that which corresponds to a depth Froude number (Fn_h) greater than 0.5, the local pressure distribution around the hull starts being directly affected by the water depth. The theoretical critical speed corresponds to Fn_h=1, this speed leads to significant growth of the bow wave and a consequent increase of the wave resistance [8] [9].

Radojcic et al. [9] state that according to ITTC 2017 [10], shallow water effects on vessel resistance should be taken into consideration when either the water depth – draught relationship (h/T) is below 4 or the depth Froude number (Fn_h) is higher than 0.5. Given the water depth levels of the Magdalena, most vessels navigating on this river will fulfil at least one of these criteria.

The shallow water resistance estimation methods consist of either giving a speed correction or a resistance correction. The method of Lackenby [11], one of the most widely known, consists of a formula that can be used to determine the speed loss in shallow waters compared to the speed in deep water [see Eq. 3].

$$V(h) = V(\infty) - \left(0.1242\left(\frac{A_{\text{m}}}{h^2} - 0.05\right) + 1 - \left(\tanh\left(\frac{gh}{V^2(\infty)}\right)\right)^{\frac{1}{2}}\right)V(\infty) \tag{3}$$

The method of Lackenby corrects the vessel speed and then, with this speed correction, resistance can be calculated by a deep water resistance method. Rottenveel [12] stated that according to a research at Marin [13], the Lackenby method for resistance correction gives a relatively high correction for wave resistance, as well as a high overall resistance estimate. Although this method does not take sinkage and trim effects into account, it is frequently used to correct resistance for shallow water effects.

The method used by SURSIM simulation software to determine inland vessel resistance starts from a deep water resistance estimation by Holtrop & Mennem or any other preferred method or trends derived from experimental methods [12]. Once the deep-water resistance is known, a correction factor is applied for shallow waters. This method might be based on the method of Lackenby, and, in the same way, does not take squat effects into account. This method was selected to estimate the shallow water effects in this synthesis model considering that the Froude number based on water depth will not be above 0.65. SURSIM presented a relation as a function of keel clearance and water depth as well as on the B/T ratio [7] [see Eq.4].

$$\frac{RT\,(h)}{RT\,(\infty)} = -0.125 + 0.875\left(KwD0 + 0.4\frac{B}{T}\;KwD1\right) \qquad (4)$$

In which:

$$KwD0 = 1 + 0.97e^{-2.74\,\mathrm{CwD}}$$

$$KwD1 = 0.75e^{-4.875\,\mathrm{CwD}}$$

$$CWD = \frac{h-T}{T}$$

Although Holtrop & Mennem [5] presented in their research a model to estimate the resistance of appendices, because of the simplicity of the algorithm and undefined variables needed, the resistance of appendices was fixed as 15% of the hull´s total resistance. An additional 15% security factor was added to the obtained total hull resistance.

The required brake power (P_B)can be obtained by relating the efficiency of the propulsion system with the effective power (P_E) [see Eq. 5 and Eq. 6]. Shallow water navigation implies a reduced clearance between the bottom of a ship and the riverbed. The water inflow to the propeller is different which leads to lower propulsive efficiency. Focused on the subcritical region, Pompée [14] stated that the propulsive efficiency might be between 20% and 50%. For this project, the propulsive efficiency was set at 35%.

$$P_E = RT\;x\;V \qquad (5)$$

$$\frac{P_E}{P_B} = \eta_{\mathrm{prop}} \qquad (6)$$

Younis et al. [6] proposed in their research an equation that may be used in the early design stage to calculate the power of conventional self-propelled inland units. The relation was developed by plotting some of the existing inland container vessels on the Nile river [see Eq. 7]

$$P_B = 0.02 * \left[V^3 * \Delta^{\frac{2}{3}}\right]^{0.841} \qquad (7)$$

2.3 Autonomy computation module

Vessel autonomy is based on the load capacity and consumption of provisions and fuel. This consumption rate is affected by the size of the crew and the length of each journey.

For the consumption of drinking water, the "Sanitation on Vessel" compendium of the World Health Organization recommends using 30 gallons per person each day and storage must be sufficient for a minimum of 2 days if a drinking water treatment plant is installed. Regarding the consumption of groceries, for this module, a ratio of daily consumption per person is implemented according to U.S Navy standards [15].

2.4 *Center of gravity and weight computation module*

Weight estimations were based on regressions developed from vessels with similar performance [6]. Because at this stage it is impossible to calculate accurately the weight of the different construction groups according to the ship work breakdown structure (SWBS) that are part of the vessel, such as structure, propulsion machinery, power generation equipment, auxiliary machinery, accommodations, and communication equipment, it is essential that a margin of error to be included in the estimate. For this study, a 5% design-build margin applied to the lightweight of the vessel is used. Displacement is expressed as the sum of lightweight (W_{light}) and deadweight (Dwt) [see Eq. 8].

$$\Delta = W_{light} + Dwt \tag{8}$$

First, lightweight is defined as the sum of the weight of the structural elements, outfitting and machinery [see Eq. 9].

$$W_{light} = W_{steel} + W_{out} + W_{m/c} + \text{Margin} \tag{9}$$

In which:

$W_{steel} = Structural\ weight$
$W_{out} = Outfitting\ weight$
$W_{m/c} = Machinery\ weight$
$Margin = 5\%\ lightweight$

Younis et al [6], in their research, presented a steel weight regression for inland container vessels, in which steel weight is shown as a function of L, B, D, draught, and block coefficient, also, because of the semi empirical nature of the regression, an additional 15% margin was applied [see Eq. 10].

$$W_{steel} = 0.097 * [C * E^{1.36}]^{0.831} \tag{10}$$

In which:

$E = L_{oa} * (B + T) + 0.85L_{oa} * (D - T)$
$C = [1 + 0.05 * (C'_B - 0.7)]$

$$C'_B = \left[C_B + \frac{(1-C_B)(0.8D-T)}{3T}\right]$$

The outfitting weight (W_{out}) is proportional to L and B. Maged [16] stated that, for inland vessels, this relation presents a proportional factor of 0.028 tonne/m^2 [see Eq. 11].

$$W_{out} = 0.028\ LB \tag{11}$$

Regarding machinery weight, Schneekluth & Bertram [7] presented that machinery weight is related to diesel engine speed in such a way that machinery weights ($W_{m/c}$) can be calculated as follows.

- Low speed diesel engines (110–140 rpm): 0.016 – 0.045 t/kW
- Medium speed diesel engines (400–500 rpm): 0.012 – 0.020 t/kW
- Type ‘V’ Medium speed diesel engines (400–500 rpm): 0.008 – 0.015 t/kW

Additionally, Sherali [17] stated that the relation among machinery weight and its brake power follows a 0.02 proportional relation [see Eq. 12] given the semi empirical nature of the relation, an additional 15% margin was applied.

$$W_{m/c} = 0.020 * P_B \tag{12}$$

On the other hand, deadweight is calculated as a function of containers transported on board. 12 tons are considered the average weight for each container. The number of modular transport elements is determined based on the number of containers along the length of the vessel, the number of containers across the beam, and the number of container levels.

In addition to the payload, other weights are added to the dead weight, such as fuel, carried water, weights associated with the crew, provisions, ballast that is not permanent, or lubricating oil.

To calculate the centre of gravity (KG) related to steel, machinery, and outfitting weights previously obtained, Younis et al. [6] in his research, presented the gravity centre of each lightweight component as a proportional coefficient of depth [see Eq. 13 to 15].

$$KG_{\text{steel}} = 0.70 * D \tag{13}$$

$$\text{KG}_{\text{out}} = 1.20\text{*D} \tag{14}$$

$$\text{KG}_{\text{m/c}} = 0.60\text{*D} \tag{15}$$

Deadweight center of gravity are defined by modular containers on deck. Then, this center of gravity is defined by depth (D), the layers of containers (N_{Layer}) and container height (hcn) [see Eq. 16] [18].

$$KG_{\text{cont}} = D + \left[\frac{N_{\text{Layer}} * hcn}{2}\right] \tag{16}$$

For centers of gravity of other weights such as fuel, provisions, drinking water, non-permanent ballast, stores or lubricating oil, [17] proposed the next relation [see Eq. 17].

$$KG_{\text{others}} = 0.34 * D \tag{17}$$

2.5 *Stability checking module*

Stability could be defined as the property of a body that causes it when disturbed from a condition of equilibrium or steady motion to develop forces or moments that finally restore the original steady condition. In vessels, a higher stability grade implies that are less prone to capsize.

The principles behind the stability of river vessels are no different from those of seagoing vessels and therefore common knowledge methods can be used to determine the stability of a vessel in river navigation. There are, however, regulations that are related to the stability of river vessels that must be followed, these regulations affect the freeboard and can limit the amount of cargo that can be transported [19].

In the early stages of design, the transverse metacentric height (GMT) indicates the level of stability of the vessel, as well for riverine vessels, the GMT must be above 1 meter [see Fig. 3] [see Eq. 18] [9].

$$GM_{\text{T}} = KB + BM_{\text{T}} - KG \tag{18}$$

Where KB is the vertical buoyancy center, BM_T is the transverse metacentric radius, KG is the vertical center of gravity. Rawson &Tupper [19] stated that KB for riverine vessels can be calculated as a function of draught [See Eq. 19].

$$KB = 0.535 * T \tag{19}$$

Similarly, the transverse metacentric radius (BM_T) is calculated according to the following equation [19] [see Eq. 20].

$$BM_T = \left[\frac{1}{12.5\text{-}\left(\frac{T}{D}\right)}\right] * \frac{B^2}{T} \tag{20}$$

The vertical center of gravity (KG) is calculated using the following equation, considering the centers of gravity calculated in the module of weights and centers of mass [see Eq. 21].

$$KG = \frac{(W*KG)_{\text{light}}+(W*KG)_{\text{Dwt}}}{\Delta} \tag{21}$$

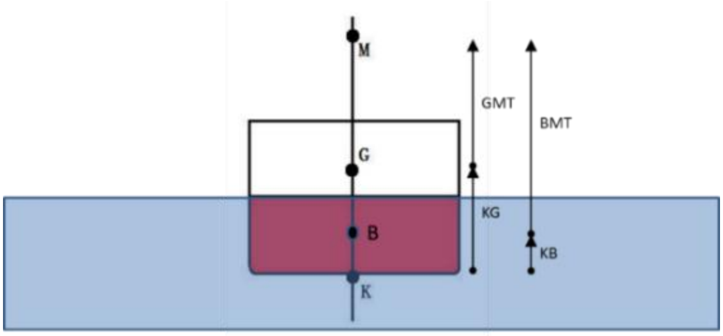

Fig. 3 Schematic of stability parameters

2.6 Cost calculation module

This module was carried out to calculate the cost required for construction (C_{Req}). The model is based on material (C_{steel}), outfitting (C_{out}) and machinery costs ($C_{\text{m/c}}$) [see Eq. 22].

$$C_{\text{Req}} = C_{\text{steel}} + C_{\text{out}} + C_{\text{m/c}} \tag{22}$$

The steel cost (C_{steel}) is defined by material (C_{smat}) and labor cost [20][see Eq. 23]. The labor cost (C_{slab}), is given as a result of man hours (Mhs_{Hull}) multiplied by the cost of each hour (Cmh_{hull}) [see Eq. 24 and 25]. K_0 is defined as a sensitivity constant obtained by each shipyard.

$$C_{\text{Steel}} = C_{\text{slab}} + C_{\text{smat}} \tag{23}$$

$$C_{\text{slab}} = Mhs_{\text{hull}} * Cmh_{\text{hull}} \tag{24}$$

$$Mhs_{\text{hull}} = K_0 * \frac{\sqrt[3]{L_{\text{oa}}*W_{\text{Steel}}^2}}{C_{\text{b}}} \tag{25}$$

The block coefficient is used as a shape factor that affects the content of the steelwork that comprises the hull shape steel in the form of one more cost to produce.

The Material Cost (C_{smat}) is calculated by multiplying the weight of the steel by a fixed value for the manufacture of one tonne of steel [20]. The cost of welding and gases is normally added to the structural material cost as a percentage which is based on an analysis of vessels previously built [see Eq. 26].

$$C_{\text{smat}} = (1 + C_0)^5 * (1 + S_v) * V_{\text{steel}} * W_{\text{steel}} \tag{26}$$

Where S_v is a waste factor and V_{steel} is the steel cost per ton, C_0 is the change in percentage of the unit cost of the material [21] .This is a function of the block coefficient, which also changes the costs of the hull and the propulsion systems.

Equipment and engineering costs are divided into labor equipment cost (C_{olab}) and equipment material cost (C_{omat}) [see Eq. 27]. Equipment labor costs are calculated from the equipment weight [see Eq. 28], which requires an evaluation of man-hours and multiplying this by an average wage per man-hour [21].

$$C_{\text{out}} = C_{\text{olab}} + C_{\text{omat}} \tag{27}$$

$$C_{olab} = Mhs_{out} + Cmh_{out} \tag{28}$$

The required Man-hours for outfitting (Mhs_{out}) are calculated from the following formula [see Eq. 29], where K_1 denotes productivity levels, salary ratios, expenses and earnings obtained by each shipyard.

$$Mhs_{out} = K_1 * (W_{out})^{\frac{2}{3}} \tag{29}$$

Equipment material cost (C_{omat}) is defined by the relationship between the equipment weight and material unit cost factors [see Eq. 30] [20]. On the other hand, propulsion plant costs ($C_{m/c}$) are assumed to vary continuously with propulsion power, and this is the result of propulsion power multiplied by unit costs per unit of energy [21].

$$C_{omat} = (1 + C_0)^5 * K_2 * (W_{out})^n \tag{30}$$

Where $n=0.95$ is related to material costs [20] and K_2 is set for the Colombian shipyard selected for the project.

3. Methodology

For this work, to run the model, a MATLAB code was developed. The algorithm is mainly composed of four blocks. In the first block, the input data corresponding to the initial dimensions between the set boundaries is entered.

In the second block, the restrictions of the dimensions that give the borders of the design space are presented Before entering the for-loop, the step of the variation of the parameters is determined to generate the possible combinations. Finally, in the block for calculations, the power modules, capacities, weights, stability, and costs are carried out; from this module, the combinations that do not meet the requirements established for each module are discarded. At the exit of this module, the iterations that make up the design space are saved [see Fig. 4].

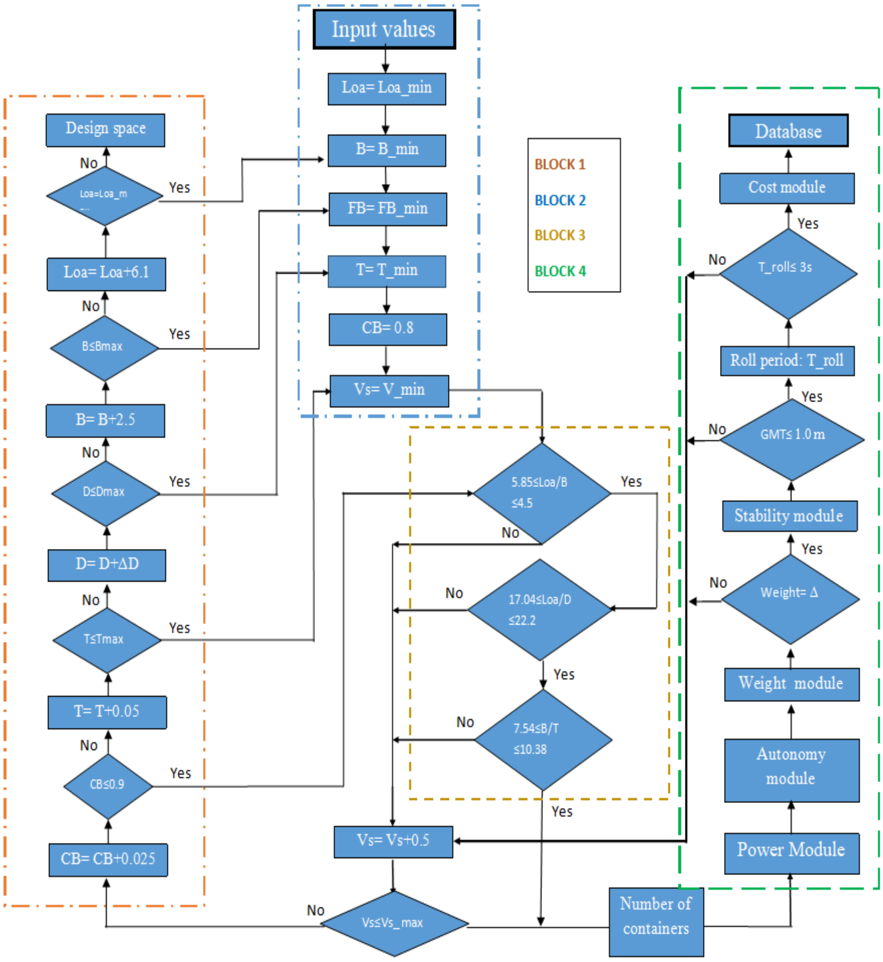

Fig. 4 Synthesis model algorithm

3.1 Boundaries of the synthesis model

To determine the main dimensions of the concept vessel, the boundaries of the possible length, beam, and depth obtained must be established. Those boundaries are defined based on parametric references of vessels with similar characteristics related to the concept vessel. For this study, the *L/B*, *L/D*, and *B/T* relationships are defined by Younis et al. [6].

Most inland vessels are characterized by high values in block coefficients and, hence, a greater displacement at the low draft and resulting in a reduction in their construction cost. Therefore, for most riverine navigation vessels, the block coefficient can vary between 0.8 and 0.9 [9].

The vessel draught is limited by the depth of the water. The clearance between the vessel and the bottom of the track must be at least 0.50 m [22]. The minimum depth established in the project requirements with a value of 2.0 m is taken as a reference. Then, the maximum design draught is to be 1.5 m. Based on the B/T ratios and the minimum freeboard constraints – 0.5 m -the minimum possible draft boundary for the vessel is found to be 1 m [see Fig. 5].

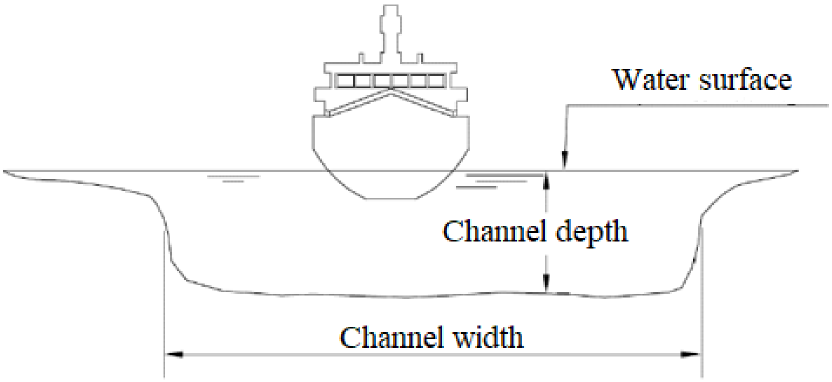

Fig. 5 Channel dimensions

The minimum channel widths necessary for safe navigation on straight sections depend on the type and size of the equipment generally used in the channel, the alignment and speed of the currents, the intensity of the prevailing wind, the limits of the channel, aids to navigation, and whether one-way or two-way traffic is allowed. The minimum width of the channel must be enough to accommodate the width of a ship, the space between the ship and the edge of the channel, and the space between ships for two-way traffic [23].

Operating experience has indicated that the minimum space required for reasonably safe navigation on straight sections should be at least 20 feet (6 meters) between the vessel and the limits of the two-way traffic channel; 40 feet (12.19 meters) for one-way traffic, and at least 50 feet (15.2 meters) between skids when passing [24].

Considering the specifications for the double-lane navigable channel of the Magdalena River with a width of 52 m in the section between Barranquilla and Barrancabermeja, the maximum beam of the vessels that would use the fluvial artery according to the safe navigation specifications must comply with the previous considerations. Therefore, the maximum possible beam of the concept vessel cannot be greater than 12.5 m [24]. Given the B/T and L/T relationships and the need to carry on board two containers in width, the minimum beam boundary is set at 7.5 m.

The depth restrictions are determined by the maximum and minimum length/depth ratios. Then, the maximum depth of the vessel could be 3.5 m and the smallest, 2.3 m [see tables 1 & 2].

Table 1 Geometric relationships

Geometric relationships	Cargo Vessels
L_{OA}/D	22.20 – 17.04
L_{OA}/B	6.5 – 4.50
B/T	10.38 – 7.54
Cb	0.8 – 0.9

Table 2 Geometric relationships

Characteristics	Cargo Vessels
Beam [m]	12.4 – 7.4
Length [m]	78.1 – 41.5
Depth [m]	3.5 – 2.5
Draught [m]	1.6 – 1.2
Vessel speed [knots]	9.0 – 6.2

4. Results and discussions

From the synthesis model, 628320 iterations were obtained, 51064 of which were convergent. For each of those convergent solutions, vessel basic geometry characteristics, such as required brake power, displacements, weights, and acquisition costs, were stored. First, the convergent results filtered on vessels capable of navigation at 9 knots were plotted in terms of brake power as a function of displacement to obtain the design space. Additional L and B relations were characterized to discuss the dimensional effect on the power/displacement relationship [see Fig. 6].

By relating the values obtained in the relation between displacement and the required brake power at 9 knots, it can be seen that the higher the displacement, the higher the brake power requirements. Additionally, each plotted point is related to a different block coefficient value from 0.8 to 0.9; the higher the value of this coefficient, the higher the displacement and the brake power required. Also, the points are grouped by length and beam, and inside these groups, each point differs from the others by depth and draught values.

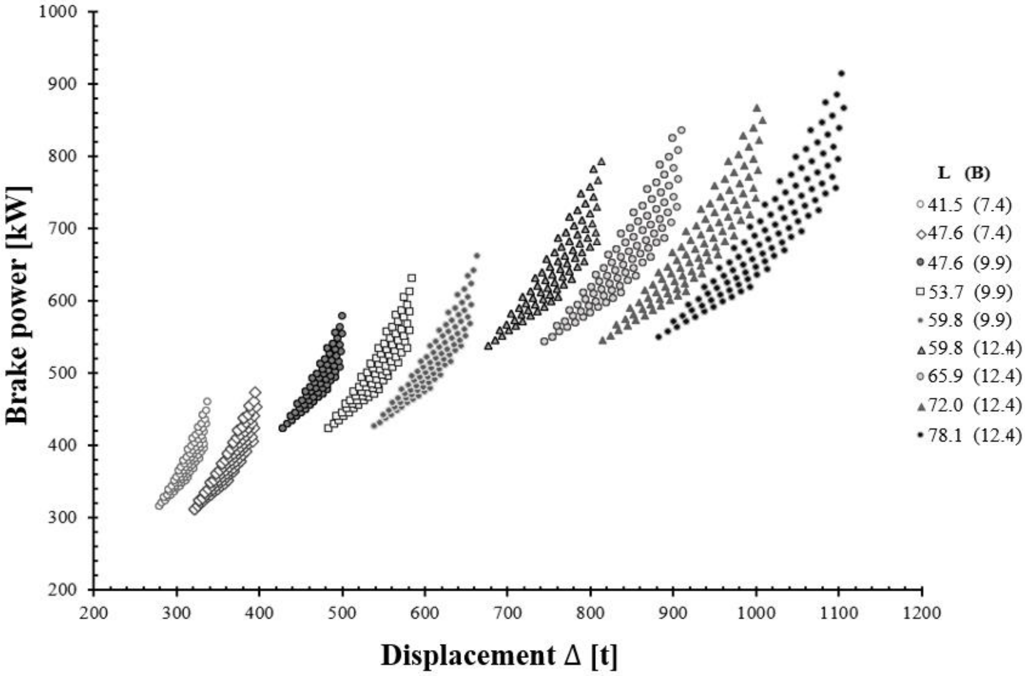

Fig. 6 Required brake power at 9 knots as function of displacement

There is a strong dependence between the increase of brake power and beam; an increase of 33% in beam implies an increase of nearly 50% in brake power. Although, an increase of 29% in length only implies an 8% growth in power brake. The trends of these were explained by [6] where it is stated that cargo riverine vessels present a flat bottom due to draught restrictions. Longer and slender vessels present lower hull resistance, while vessels designed with a wider beam are known for better stability.

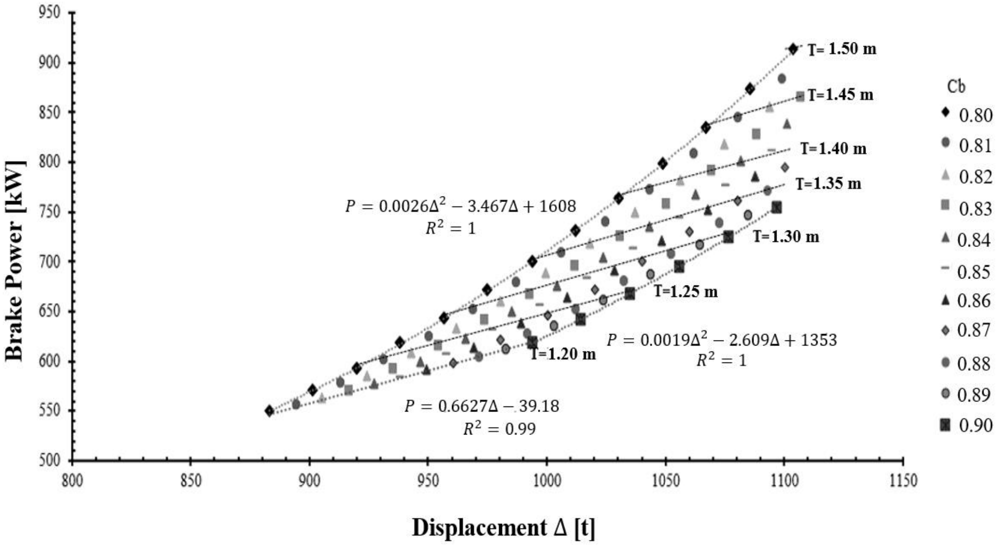

Fig. 7 Required brake power at 9 knots at 78.1 m length and 12.4 m beam

With the set of results related to 78.1 m length and 12.4 m beam, the characteristics of the global obtained data will be explained as a function of block coefficient (C_b) and draught (T) [see Fig. 7]. An increase in block coefficient would imply a proportional growth in displacement and, hence, an increase in brake power. According to the analytic models, the relationship between displacement and brake power fits in a quadratic regression, and, after classifying the results as a function of block coefficient and draught, it was found that draught, given the theoretical and semi-empirical model exposed, has a higher influence in the behaviour of brake power than block coefficient. For instance, an increment of 12.5% in C_b, would imply a 20% growth in brake power whereas an 8% increment in draught would bring as consequence an increase of 21% in brake power.

The effect of draught and block coefficient on power brake and displacement can be evaluated in the next graph [see Fig. 8].

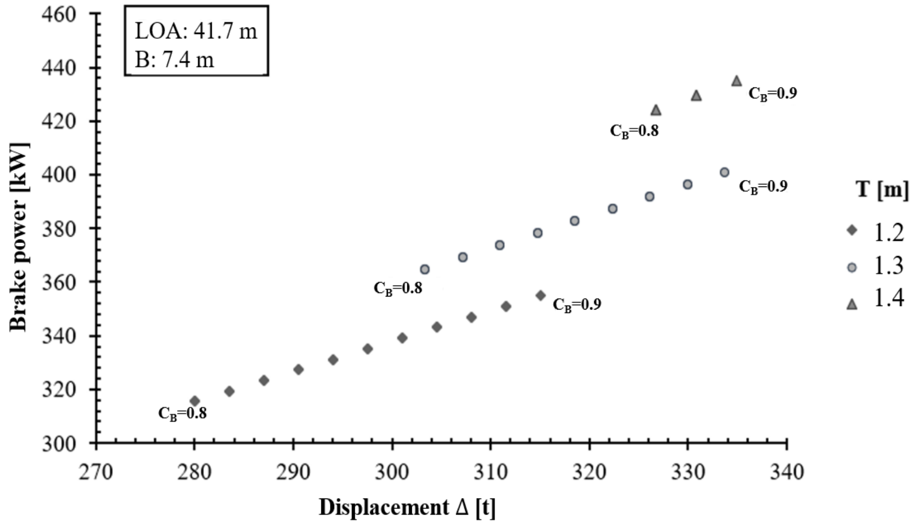

Fig. 8 Effect of draft in brake power- displacement relationship

To evaluate the effectiveness of a riverine cargo vessel, it is deemed necessary to know how many deadweight tons are displaced by each power unit. Thus, a relationship between the brake power and deadweight ratio as a function of the ratio between lightweight and displacement has been proposed. The obtained data are segregated by length and beam [see Fig. 9].

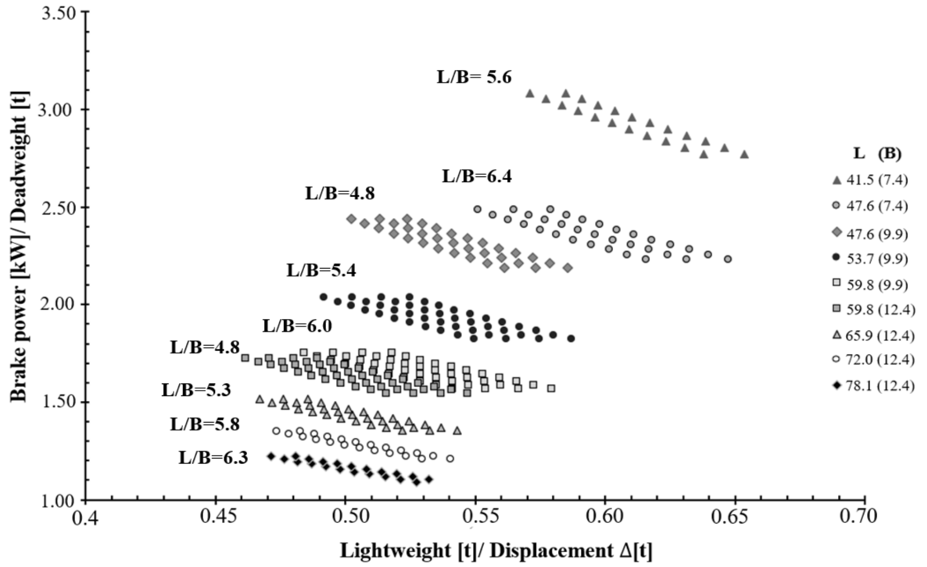

Fig. 9 Brake power – deadweight ratio vs displacement ratio at 9 knots and 1.2 m draught

Displacement is the consequence of the summation of deadweight and lightweight [see eq. 6]. Figure 9 shows that an increase in length implies a reduction in the lightweight-displacement ratio and, hence, a larger proportion of deadweight in the displacement. Additionally, at the same beam, longer and slender vessels entail a lower requirement of braking power for each tonne of deadweight. For instance, with 12.4 m of beam, an increase of 19% in L/B ratio implies a reduction of nearly 20% in brake power requirements per tonne of deadweight.

Vessels with smaller beams have a higher proportion of lightweight with regard to their displacement. For example, when vessels of 41.5 m and 78.1 m of length are compared, the lightweight of the vessel can represent up to 65% of the displacement, while for the latter, the lightweight represents between 43% and 53% of the displacement. These percentages could be a consequence of the limited draught established.

As a complement to the previous graph, the effect of draught on the brake power/deadweight ratio is presented below [see Fig. 10]. An increase in draught leads to a proportional rise in the required power. The increase in power required for each tonne of cargo would increase by up to 35% with only a 16% increase in draught.

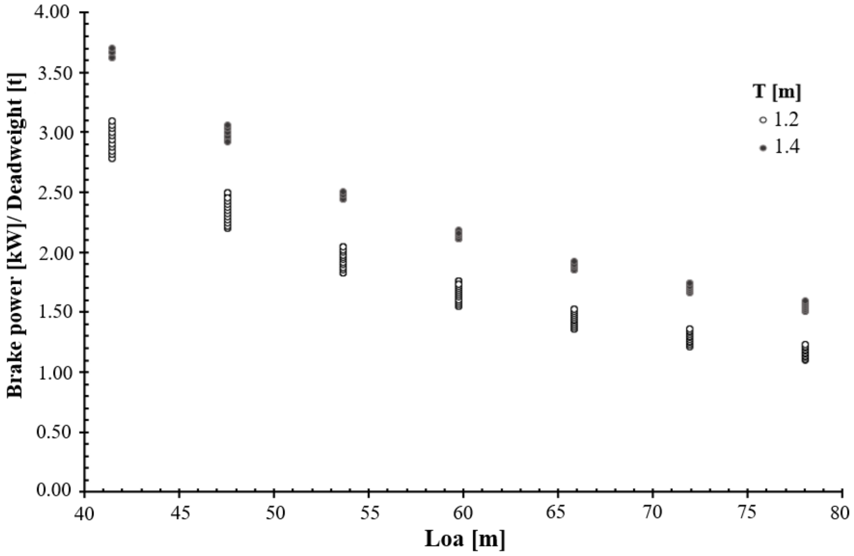

Fig. 10 Effect of draft on brake power-deadweight ratio

Next, the effect of depth in lightweight is analyzed. The increase in depth may lead to a slightly rise in steel weight. A depth elongation of 16% leads to an increase up to about of 2.5% in lightweight [see Fig. 11].

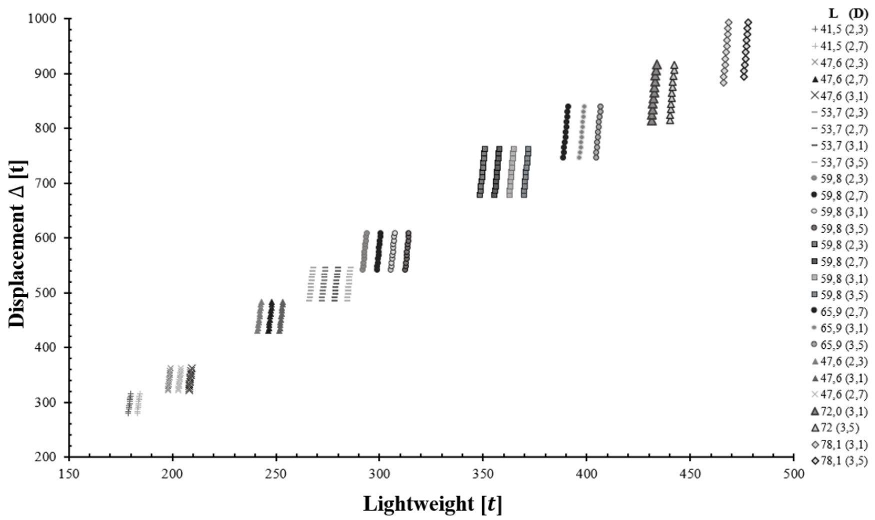

Fig. 11 Effect of depth on displacement

According to the previously described relationships, and to obtain the most convenient conceptual solution, a multi-criteria selection model was developed with the 'Expert Choice' software to define the measures of merit criteria. This software, by implementing an analytical hierarchy process, allows the selection of one of the alternatives. As criteria for choosing the best alternative, the deadweight, the weight, the range, and the minimum required brake power were used.

A vessel capable of carrying the greatest number of supplies with the lowest power requirements, draught and lightweight is desirable for this project. A greater range would allow reaching more remote locations and a lower power requirement would allow the selection of engines with decreased weight, consumption, and dimensions, even ensuring a maximum speed of 9 knots. Using the selection model, the best-ranked solutions are calculated according to the following measure of merit [see table 3]. The percentages represented in the measure of merit show the preponderance of each described parameter in the selection of the vessel over 100%

Table 3 Measure of merit of the selection model

Parameter	Measure of merit
Deadweight	*38.8%*
Min. Brake power	*31.1%*
Draught	*14.3%*
Lightweight	*10.4%*
Range	*5.4%*

Given the variable conditions of the Magdalena river, the size of ports and piers, and the functionality of the vessels, a unique optimal vessel found may not be appropriate for the most common transportation functions and available port infrastructure. Therefore, three sets were formed with the results based on their beam [see Fig. 7] and, from each set, a vessel was obtained that would effectively satisfy the design requirements [see Fig. 12]. The greater the reported percentage, the better the performance in each parameter.

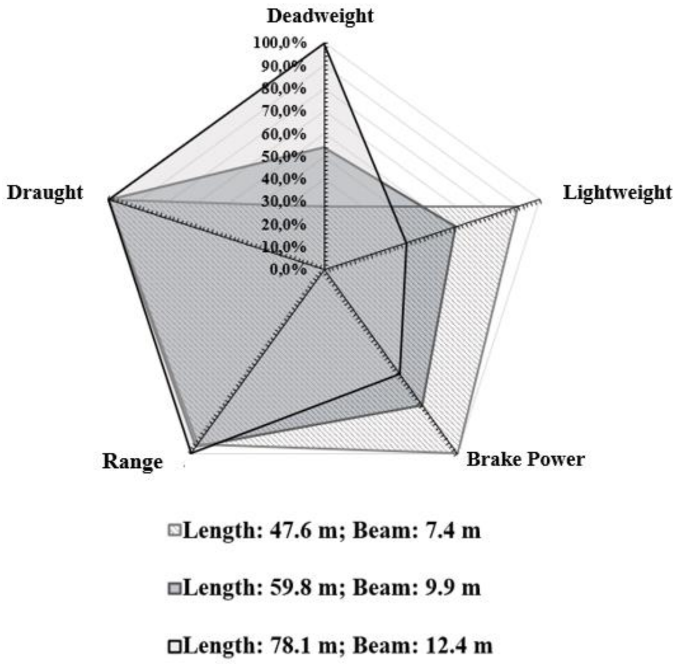

Fig. 12 Best ranked solutions performance

The rating recorded for each of the parameters in the above graph refers to the overall data. The vessel, with a length of 78.1 m and a beam of 12.4 m, has an overall rating in terms of the deadweight of 99.5%, being surpassed only by vessels with a higher block coefficient. Similarly, the 47.6 m long vessel with a beam of 7.4 m presents the global minimum of required power. Given the hierarchy of the chosen parameters, the vessel with the greatest length and beam would represent the best overall rated option.

When relating the cost of acquisition to the length of the vessel, it is found that the alternative with the shortest length represents the highest cost of acquisition per length [see Fig. 13]. This relationship would be related to the price of steel and the lightweight/displacement ratio. On the other hand, when the minimum power required is related to the deadweight regarding the three chosen alternatives, it was found that less power is required to move each tonne of deadweight at longer vessel lengths [see Fig.14].

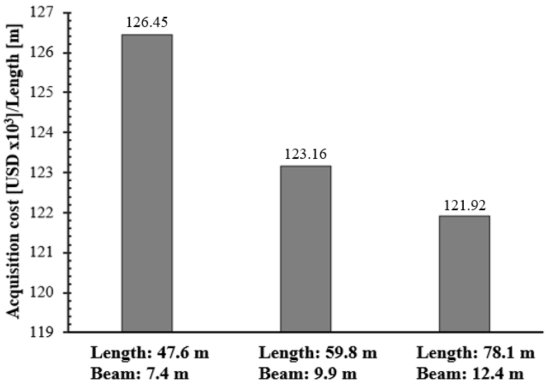

Fig. 13 Acquisition cost- best ranked solutions

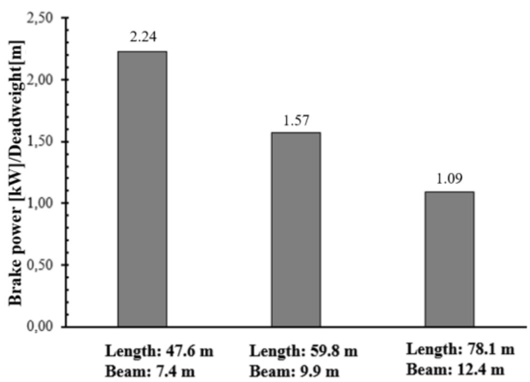

Fig. 14 Brake power- best ranked solutions

The figure below shows the power curve for the three selected alternatives as a function of the relative speed of the vessel. The vessel with the largest length has the highest power requirement given the strong influence of beam in the power required [see Fig. 15].

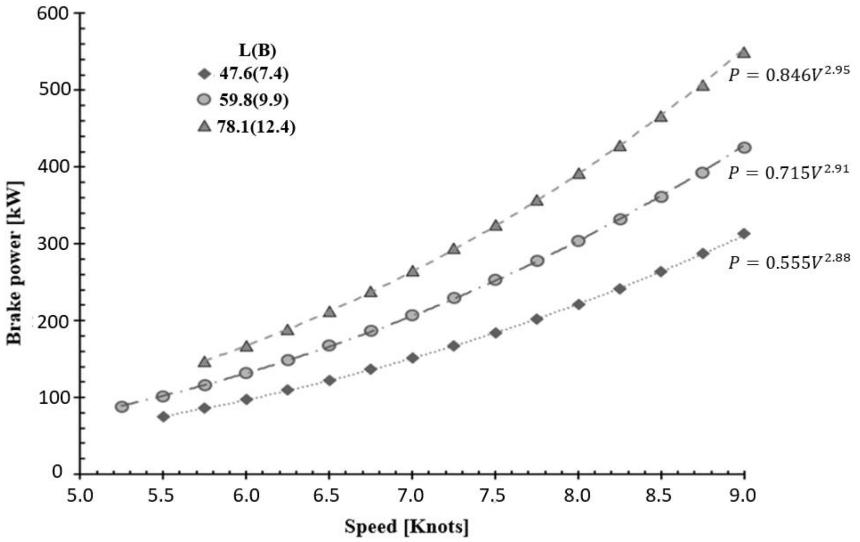

Fig. 15 Best ranked solutions performance at deep waters

The characteristics of the three best ranked solutions are exposed in the next table [see table 4]. Each alternative represents solutions to different requirements related to deadweight and range needed.

Table 4 Conceptual vessel models selected

Dimensions	Alternative 1	Alternative 2	Alternative 3
Length overall (LOA)	47.60± 3 m	59.80± 3 m	78.10± 3 m
Length at the waterline (LWL)	45.22± 3 m	56.81± 3 m	74.19± 3 m
Beam (B)	7.40 ± 1,25 m	9.90 ± 1.25 m	12.40± 1.25 m
Depth (D)	2.30 m	2.30 m	3.10 m
Draught (T)	1.20 m	1.20 m	1.20 m
Brake power (9 knots)	312.85 kW	425.49 kW	549.32 kW
Deadweight	140.32 t	271.26 t	503.47 t
Lightweight	178.02 t	263.03 t	379.75 t
Displacement	318.34 t	534.29 t	883.22 t
KG [m]	2.31 m	2.43 m	2.82 m
Block Coefficient (Cb)	0.8	0.8	0.8

The conceptual designs of the proposed vessels are partially based on logistic support vessels and landing crafts commissioned by the Colombian navy and designed by COTECMAR [see Fig. 16 to 18]

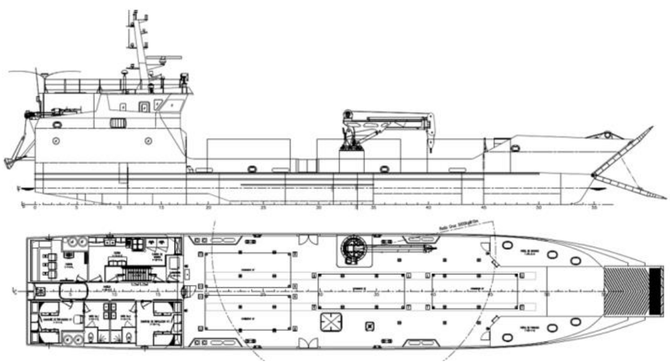

Fig. 16 Proposed conceptual design of the alternative 1

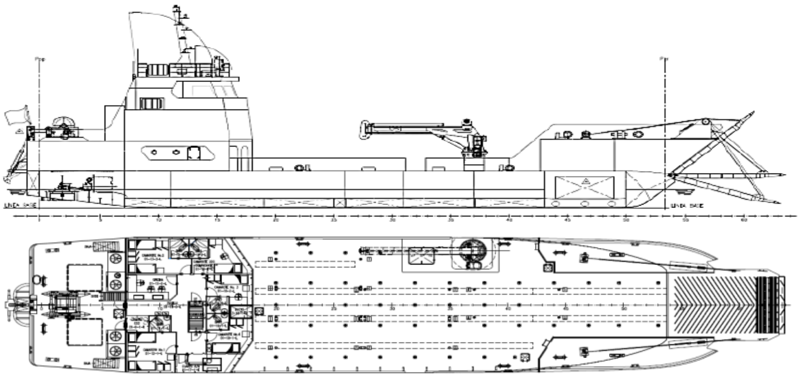

Fig. 17 Proposed conceptual design of the alternative 2

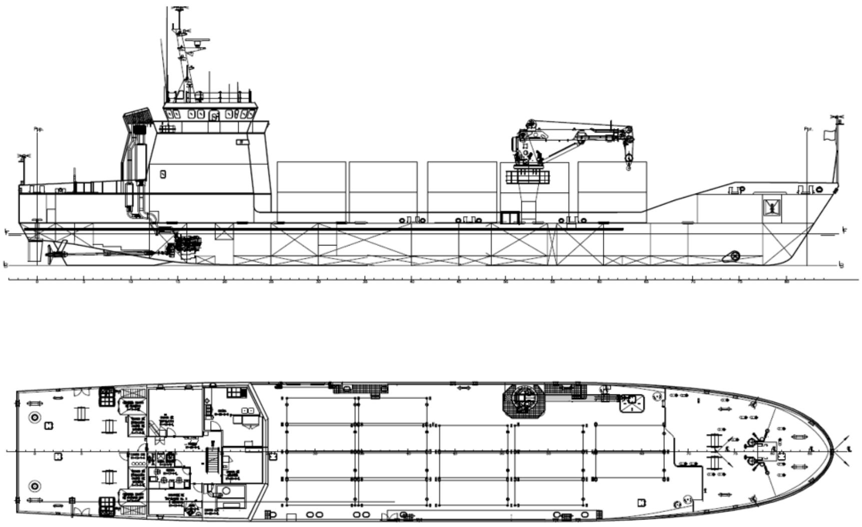

Fig. 18 Proposed conceptual design of the alternative 3

5. Validations of the synthesis model

To validate the model, a riverine low draft logistic support vessel, designed by COTECMAR to provide medical and humanitarian aid, was taken as a reference. [see Fig. 19]. For validation of the model's modules, the dimensions and main characteristics of the reference vessel were taken as inputs [see table 5].

Fig. 19 Reference vessel to validate the synthesis model

Table 5 Main Dimensions of the reference validation vessel

Dimensions	Reference vessel
Length overall (LOA)	43.40 m
Length at the waterline (L)	40.2 m
Beam (B)	8.0 m
Depth (D)	2.30 m
Draught (T)	1.20 m
Installed Brake power	448 kW
Displacement	313.2 t
Shallow waters speed	6 kn
Deep waters speed	8 kn
Block Coefficient	0.812

5.1 Validation of the weight module

According to Table 6, the lightweight of the reference vessel is represented by the synthesis model with an error margin of 5.82%. The lowest difference is found in the structural weight calculations [see eq. 8] with a difference of 5.12% and the highest is represented by machinery weight [see eq. 10].

Table 6 lightweight of the vessel in comparison with the synthesis model

Dimensions	Reference vessel	Synthesis Model	Difference [%]
Structural weight (W_{steel})	114.9 t	109.3 t	5.12%
Outfitting weight (W_{out})	70.34 t	62.73 t	10.8%
Machinery weight ($W_{m/c}$)	12.60 t	10.61 t	15.7%
Lightweight (W_{light})	197.84 t	186.32 t	5.82%

5.2 Validation of the resistance and powering module

The total hull resistance of the reference vessel was studied with experimental models. Experimental model tests have been performed in the Towing Tank of the Universidad Austral de Chile at waveless deep and shallow water conditions [see Fig 20]. The parameters of these tests are showed in Table 7.

Table 7 Towing tank test parameters

Parameters	Reference vessel
Scale (λ)	20
Tank water temperature (T_w)	20°C
Water density (ρ)	1005 kg/m^3
Kinematic viscosity (ν)	1.04x10^{-6} m^2/s

Fig. 20 Towing tank tests with the model of the reference vessel

From the test, it was obtained a total resistance and effective power curve at shallow and deep water conditions. The effective power was set up with the propulsive efficiency, detailed in section 2.2. These curves were compared with resistance vs speed curves obtained by the proposed model and Holtrop-Mennen resistance model, all with corrections by the SURSIM method for shallow water resistance. The Younis model [see Eq. 7] was also compared in brake power curves.

The comparison of the models with the towing tank resistance results shows two different behaviours. On one side, at deep water conditions, the synthesis model formulation presents an error of 6.53% concerning experimental results of the functional design speed whereas at the same point, Holtrop-Mennem method exhibit an error close to 23% [see Fig 21]. Nevertheless, at higher speeds than the functional design speed, both models underestimate the ship resistance, and, consequently, the brake power required [see table 9].

Experimental results also showed that at higher speeds than 8 knots in deep water conditions, there is a considerable increase in sinkage. In brake power estimations, the synthesis model formulation exhibits an error of 5.1% at the functional design speed whereas Holtrop-Mennem method underestimates the needed brake power by 22.7% and Younis method overestimates the brake power showing a difference of 82% according to the experimental results [see table 10] [see Fig 22].

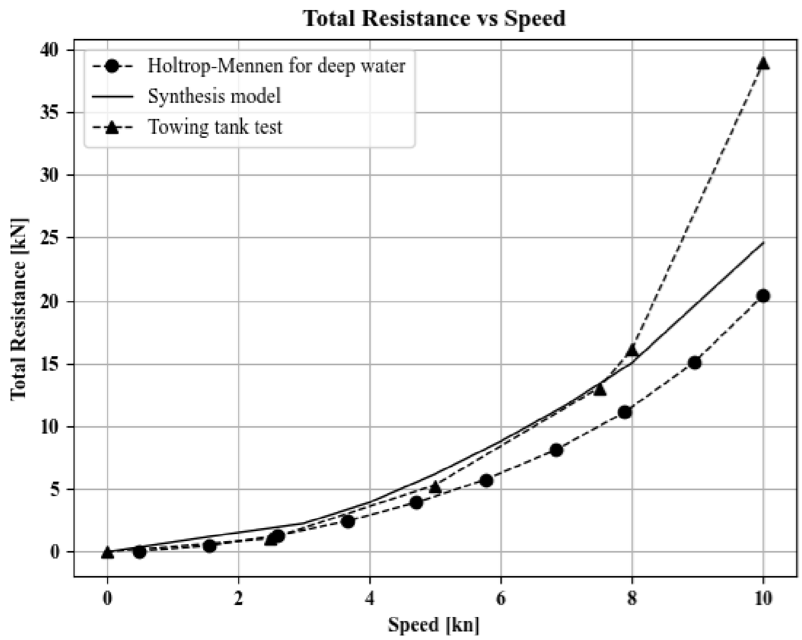

Fig. 21 Total Resistance related to Ship Speed at deep waters conditions

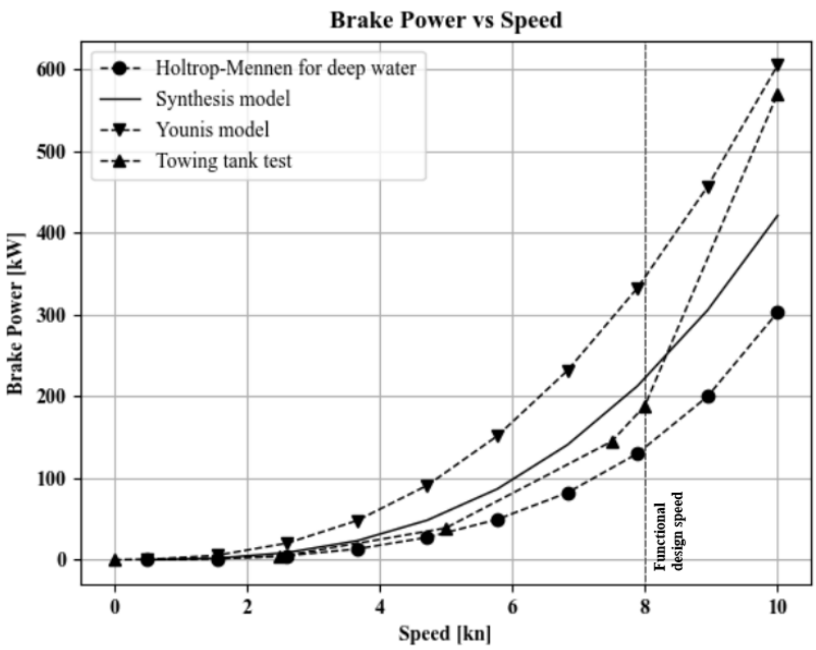

Fig. 22 Brake Power related to Ship Speed at deep waters conditions

On the other hand, in shallow water conditions, both models present coherence with the trends of the experimental results until the depth Froude number reach a value near 0.6. The approach proposed in the synthesis models obtains errors below to 6% until the previously mentioned depth Froude number [see Fig 23]. After that point, resistance and consequently the required brake power showed a drastic increment [see table 10]. This behaviour could be explained due to the transition from the sub-critical region to the critical region, where the effects of water depth strongly affect the wave-making resistance [see Fig 24].

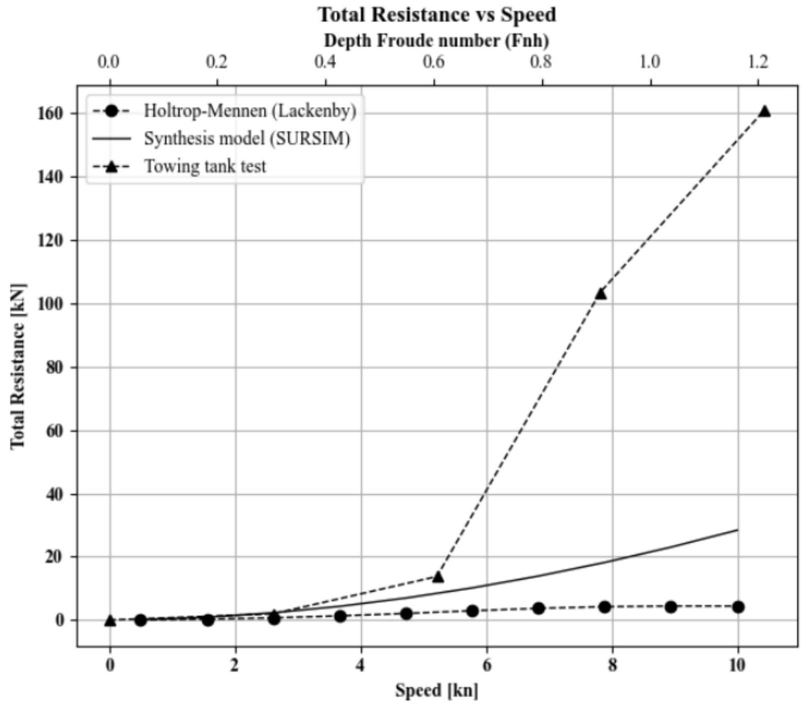

Fig. 23 Total Resistance related to Ship Speed at shallow waters conditions

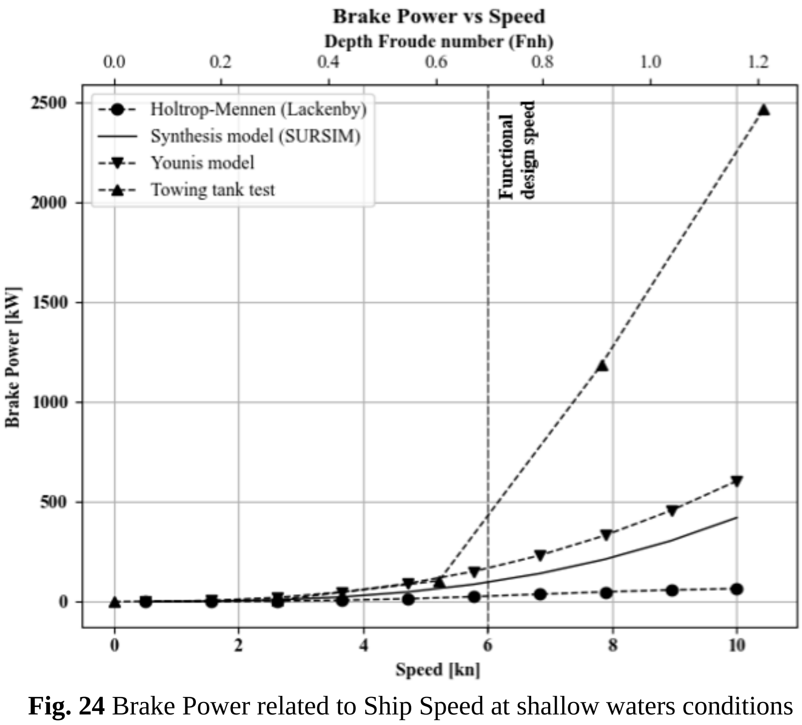

Fig. 24 Brake Power related to Ship Speed at shallow waters conditions

Table 9 Total hull resistance in comparison with the synthesis model and Holtrop-Mennem model

	Towing tank test	**Synthesis Model**		**Holtrop-Mennem**	
Resistance	**values**	**values**	**difference**	**values**	**difference**
Deep Water Resistance at 8 kn	16.08 kN	15.03 kN	6.53%	12.4 kN	22.88%
Deep Water Resistance at 4 kn	3.51 kN	3.92 kN	10.45%	2.98 kN	15.09%
Shallow water resistance at 6 kn	39.87 kN	10.58 kN	73.46%	6.36 kN	84.04%
Shallow water resistance at 5 kn	8.32 kN	7.44 kN	10.57%	5.88 kN	29.3%
Shallow water resistance at 3 kn	2.67 kN	2.72 kN	1.87%	2.45 kN	8.23%

Table 10 Brake power in comparison with the synthesis model and Holtrop-Mennem model

	Towing tank test	**Synthesis Model**		**Holtrop-Mennem**		**Younis**	
Brake power	**values**	**values**	**difference**	**values**	**difference**	**values**	**difference**
Deep Water brake power at 8 kn	188.64 kW	203.19 kW	5.12%	145.79 kW	22.7%	343,83 kW	82.22%
Deep Water Brake power at 4 kn	24.97 kW	26.53 kW	6.41%	17.51 kW	29.8%	67.52 kW	170.04%
Shallow water brake power at 6 kn	429.21 kW	107.26 kW	75.0%	56.08 kW	86.93%	231.14 kW	46.14%
Shallow water brake power at 5 kn	61.11 kW	52.19 kW	5.82%	43.21 kW	29.29%	58.92 kW	3.58%
Shallow water brake power at 3 kn	11.26 kW	11.47 kW	1.86%	10.80 kW	4.08%	12.33 kW	9.50%

6. Conclusions

With the development of this rational methodology, a convergent and adequate solution is obtained of the conceptual design for a riverine cargo vessel based on the requirements and restrictions of inland navigation on the Magdalena River.

The design space corresponds to viable alternatives for a riverine cargo vessel. This design space can be dimensioned by means of synthesis models whose parameters, limits and restrictions are determined by semi-empirical approximations, regressions and analytical relationships. From this model, the dimensions for three 1.2 m draught vessels with different deadweight/lightweight ratios and installed power requirements were obtained. The obtained vessel dimensions can be the design baseline for subsequent designs.

The required brake power is strongly influenced by the beam and the length/beam ratio in the second instance. A decrease in L/B ratio implies that longer and slender vessels present less brake powering requirements per tonne of deadweight. Block coefficient presents a slighter influence in brake powering requirements in comparison with the effect of draught.

Acknowledgements

The authors are very grateful for the constant support of the Science and Technology Corporation for Naval, Maritime and Riverine Industry Development (COTECMAR), and the funding provided by the Ministry of Science, Technology and innovation (Minciencias) and the Mining-Energy Planning Unit.

REFERENCES

[1] Ministerio de Transporte., 2018. Situación de la infraestructura y el transporte Fluvial en Colombia. Superintendencia de puertos y transporte. Bogotá DC, Colombia.

[2] Kerns, C., 2011. Naval Ship Design and Synthesis Model architecture using a model-based systems engineering approach. Master thesis.Virginia polytechnic Institute. Blacksburg, Virginia.

[3] Vernego, G., Rizzuto, E., 2014. Vessel synthesis model for the preliminary desigh of a fleet of compressed natural gas carriers., *Ocean Engineering*, 89, 188-199. https://doi.org/10.1016/j.oceaneng.2014.08.012

[4] Yuanhang, H., Zhang, J., Chunbo, Z., 2014. Development of naval ship synthesis model in concept design, *Advanced Materials Research*, 1, 2945-949, pp. 490-493. https://doi.org/10.4028/www.scientific.net/AMR.945-949.490

[5] Holtrop, J., Mennem, F., 1982. An approximate power prediction method, *International Shipbuilding Progress*, 29, 166-171. https://doi.org/10.3233/ISP-1982-2933501

[6] Younis, G., Gafaary, M., El- Kilani, H., Moustafa, M., 2011. Techno-Economical Optimization for River Nile Container Ships. *Brodogradnja*, 62(4), pp. 383-395.

[7] Schneekluth, H., Bertram,V., 1998. Vessel Design for Efficiency and Economy, Butterworth Heinemann. https://doi.org/10.1016/B978-075064133-3/50002-5

[8] Molland, A. Turnock, S., Hudson, D., 2011. Ship Resistance and propulsion: Practical estimation of ship propulsive power (1st ed), Cambridge University Press. https://doi.org/10.1017/CBO9780511974113

[9] D. Radojcic, A. Simic, N. Momcilovic, M. Motok y B. Friedhoff., 2021. Design of Contemporany Inland Waterway Vessels: The case of the Danube River, Belgrade: Springer. https://doi.org/10.1007/978-3-030-77325-0

[10] ITTC. 2017. Recommended procedures and Guidelines -1978 Performance prediction method. 7.5-02-03-01.4 Propulsion Committe of the 28th, ITTC.

[11] Lackenby, H.,1963. The effect of shallow water on ship speed, The ship builder and the marine engine builder. *Naval Engineers Journal*, 76(1), 21-26 https://doi.org/10.1111/j.1559-3584.1964.tb04413.x

[12] Rotteveel, E., 2013. Investigation of inland ship resistance, propulsion and manoeuvring using literature study and potential flow calculations, Delf: TU Delf.

[13] Raven, H., 2012. Towards a new shallow-water correction method for ship speed-power relations. Technical report. MARIN.

[14] Pompée, P., 2015. About modelling inland vessels resistance and propulsion and interaction vessel-waterway -Key parameters driving restricted shallow waters effects, Buenos Aires: PIANC Smart Rivers.

[15] USN., 1996. NAVSEA S9086-C6-CTM-010/CH-096R1: chapter 96: Naval Ships, Technical Manual, Weights and Stability.

[16] Maged, M., 2008. A design Optimization Model for Inland Water Units, Alexandria : Ph.D Thesis, faculty of Engineering, Alexandria University.

[17] Sherali, H., 2001. Global of the Nonconvex Containership design problem using the Reformulation-Linearization Technique, Virginia Polytechnic Institute. Virginia.

[18] German Insurance Association., 2021 Container Handbook: Cargo loss prevention information from German marine insurers, GDV.

[19] Rawson, K., Tupper, E., 2001. Basic Ship Theory, Volume 1 Ship Dynamics and Design, BH. https://doi.org/10.1016/B978-075065398-5/50004-2

[20] Hekkenberg, R., 2012. Inland ships for Efficient Transport Chains. Delf: TuDELF.

[21] Carreyette, J., 1978. Preliminary Ship Cost Estimation, *Royal Institution of Naval Architects*. Naval architect Issue: 4, pp. 235-258. ISSN: 0306-0209.

[22] Radojcic, D., 2004. Innovative Transport Vehicles on the Danube and Its Tributaries, Belgrade : Danube Project Centre.

[23] U.S Army Corps of Engineers., 1997. Engineer Manual 1110-2-1611-layout and Design of shallowdraft waterways.

[24] COTECMAR., 2015. Restricciones para el diseño de un sistema de transporte intermodal de contenedores a traves del río magdalena, COTECMAR , Cartagena , Colombia.

Submitted: 25.05.2022.
Accepted: 01.09.2022.

David Ricardo Alvarado,dalvarado@cotecmar.com
COTECMAR
Luis Alejandro Paternina, lpaternina@cotecmar.com
COTECMAR
Edwin Giovanny Paipa, lpaternina@cotecmar.com
COTECMAR